



This is a repository copy of *Influence of remote laser cutting on magnetic loss and mechanical properties in 0.2 mm silicon steel*.

White Rose Research Online URL for this paper:

<https://eprints.whiterose.ac.uk/225402/>

Version: Published Version

---

**Article:**

Jones, L.M. [orcid.org/0000-0001-9927-0913](https://orcid.org/0000-0001-9927-0913), Winter, A. [orcid.org/0000-0001-6582-149X](https://orcid.org/0000-0001-6582-149X), Tinkler, L. [orcid.org/0000-0002-8275-3967](https://orcid.org/0000-0002-8275-3967) et al. (2 more authors) (2024) Influence of remote laser cutting on magnetic loss and mechanical properties in 0.2 mm silicon steel. *Journal of Magnetism and Magnetic Materials*, 607. 172400. ISSN 0304-8853

<https://doi.org/10.1016/j.jmmm.2024.172400>

---

**Reuse**

This article is distributed under the terms of the Creative Commons Attribution (CC BY) licence. This licence allows you to distribute, remix, tweak, and build upon the work, even commercially, as long as you credit the authors for the original work. More information and the full terms of the licence here:

<https://creativecommons.org/licenses/>

**Takedown**

If you consider content in White Rose Research Online to be in breach of UK law, please notify us by emailing [eprints@whiterose.ac.uk](mailto:eprints@whiterose.ac.uk) including the URL of the record and the reason for the withdrawal request.



[eprints@whiterose.ac.uk](mailto:eprints@whiterose.ac.uk)  
<https://eprints.whiterose.ac.uk/>



## Research article

# Influence of Remote Laser Cutting on Magnetic Loss and Mechanical Properties in 0.2 mm Silicon Steel

L.M. Jones<sup>a,\*</sup>, A. Winter<sup>b</sup>, L. Tinkler<sup>b</sup>, G.W. Jewell<sup>c</sup>, H. Ghadbeigi<sup>a</sup><sup>a</sup> University of Sheffield, Department of Mechanical Engineering, Sheffield, S1 3JD, United Kingdom<sup>b</sup> University of Sheffield, Advanced Manufacturing Research Centre, Factory 2050, Europa Avenue, Sheffield, S9 1ZA, United Kingdom<sup>c</sup> University of Sheffield, Department of Electrical Engineering, Sheffield, S1 3JD, United Kingdom

## ARTICLE INFO

## Keywords:

Silicon steel  
Electrical steel  
Remote laser cutting  
Specific loss  
Fracture  
Fatigue

## ABSTRACT

Energy loss due to eddy current generation is a significant factor in reduced efficiency of electrical machines, therefore motor cores with thinner sheets are required due to their effect in reducing eddy currents. However, reducing the thickness of laminations is challenging due to the high tooling costs in blanking due to the small tolerances required, whilst other methods such as conventional laser cutting are too slow to be commercially viable. In this paper the influence of remote laser cutting on thin electrical steel sheets (Cogent/Tata Steel NO20 3.2% Si) has been investigated on the tensile strain to fracture, fatigue life, edge hardness, and energy loss in an AC magnetisation cycle for two laser power levels. The laser power has found to have no statistically significant influence on the bulk mechanical properties of the material, but significantly affects the measured specific loss. The latter was associated with the increased edge hardness at higher laser powers. Based on the parameters selected it is highly questionable whether RLC offers a viable method for lamination cutting, significant refinement of the laser parameters and/or the use of an alternative laser such as an ultra-fast pulsed laser is required to be competitive with existing methods. Additionally, it is shown that energy loss increases linearly with respect to length of the cut edge - to the minimum cut spacing tested of 6 mm. These results can be used to optimise laser parameters to reduce the degradation of magnetic properties by decreasing laser power where possible.

## 1. Introduction

The cores of electrical machines are typically made from many hundreds of individual thin sheet or laminations of silicon steel. The presence of a ferromagnetic core significantly enhances the airgap flux density and hence increases torque, while electrically isolated laminations dramatically reduce eddy current losses in comparison to a solid core. Typical lamination thicknesses are in the range of 0.05 mm to 0.65 mm, and higher operational frequencies demand thinner gauge sizes. Commercial production of 0.2 mm thicknesses is now common [1]. With the general trend towards thinner laminations to gain better functional performance, conventional stamping methods become more challenging because of the associated difficulties in handling thin and brittle parts as well as significant difficulties in manufacture of tooling which requires a die-punch clearance of 2%–10% of the sheet thickness [2]. Other cutting methods such as conventional laser cutting (CLC) have been widely used and reported in the literature, particularly for prototyping and low to medium volume manufacture. In contrast

to the speed of gantry-type CLC systems (which is typically limited to  $0.3 \text{ m s}^{-1}$  to  $0.5 \text{ m s}^{-1}$  due to the inertia of the system), the low inertia of the galvanometer in remote laser cutting (RLC) affords greater acceleration and higher speeds thus presenting a potential alternative commercially scalable manufacturing method.

While commercially available CLC has been widely researched, there is limited knowledge available on RLC and its effect on the quality of the produced parts. RLC cannot rely on an assist gas to remove molten material as in CLC, and must vaporise the material instead. This requires a beam with much higher power density, on the order of  $10^7 \text{ W cm}^{-2}$  to  $10^{10} \text{ W cm}^{-2}$  used in several successive passes at high speed ( $>1 \text{ m s}^{-1}$ ) to cause vaporisation of a proportion of the thickness in each pass [3]. These repeated scans remove tens of microns from the material per pass while cutting through the thickness of the sheet [4].

Laser cutting processes are also known to severely deteriorate the magnetic performance compared to other conventional processing routes, and it was proposed that this thermal deterioration is due

\* Corresponding author.

E-mail addresses: [l.jones@sheffield.ac.uk](mailto:l.jones@sheffield.ac.uk) (L.M. Jones), [a.i.winter@sheffield.ac.uk](mailto:a.i.winter@sheffield.ac.uk) (A. Winter), [l.tinkler@amrc.co.uk](mailto:l.tinkler@amrc.co.uk) (L. Tinkler), [g.jewell@sheffield.ac.uk](mailto:g.jewell@sheffield.ac.uk) (G.W. Jewell), [h.ghadbeigi@sheffield.ac.uk](mailto:h.ghadbeigi@sheffield.ac.uk) (H. Ghadbeigi).

<https://doi.org/10.1016/j.jmmm.2024.172400>

Received 2 February 2024; Received in revised form 11 July 2024; Accepted 31 July 2024

Available online 6 August 2024

0304-8853/© 2024 The Authors. Published by Elsevier B.V. This is an open access article under the CC BY license (<http://creativecommons.org/licenses/by/4.0/>).

to thermally induced stresses [5,6]. In this context, controlling the thermal energy input due to the laser processing is essential to reduce adverse effects on magnetic performance and cut-edge quality. Paltanea et al. [5] demonstrate that poor thermal management as a result of high heat flux into the part can negate any benefit of using thinner laminations. The thermal energy input to the material is not necessarily directly proportional to the processing parameters such as number of passes and power density. Winter et al. [4] reported microstructural alterations such as recast and heat affected zone formation due to RLC in a 0.15 mm thick Hipercob 50 cobalt iron sheet with varied powers and speeds. The authors indicated that fluence was the dominant factor in material removal rate, although a marginal increase in removal rate was also observed with increased scan speeds.

The thermal energy input from the beam may have a greater impact on thin laminations due to the presence of less thermal mass to dissipate the heat. Therefore, a thorough understanding of the thermally induced damage in thin gauge electrical lamination is essential to gain full commercial benefit of emerging laser technologies. This becomes more significant for RLC as the failure to fully vaporise material will generate significant additional heat input to the cut edge. CLC has been shown to change the microstructure at the cut edge in semi processed non grain oriented silicon steel [7], however fully processed material (i.e. annealed) does not exhibit a difference in microstructure.

The operational conditions of electrical machines are such that cyclic thermo-mechanical stresses in the laminations are unavoidable due to the heat and centrifugal forces [8]. Thinner laminations are preferred for higher-speed and thus higher-frequency applications, which result in larger mechanical stresses, mostly tensile, especially with stress concentrations at the critical geometrical features. There is not yet a comprehensive understanding on effect of cut edge properties and processing parameters on the mechanical fatigue of electrical materials. Silicon steels are the most common material used for electric machines and it is reported to be exceptionally resistant to fatigue loading, with normalised stress amplitudes as high as 0.42 with peak stresses at or above yield strength [9–11]. For thin electrical steel sheet, it was found that there was a significant effect on fatigue life due to test setup and specimen geometry [10]. This is of particular importance for hourglass specimens where the volume of material subject to a homogeneous stress state is very small, however, increasing this volume makes the sample much more likely to buckle. Gottwalt et al. [10] therefore presented several methods for fatigue testing in compression and tension using a restraint device, designed to reduce the influence of geometry and prevent buckling.

A study of 0.23 mm thick sheet specimens produced by punching showed no fatigue failure below a normalised yield strength of 1.0 at  $10^6$  cycles, where the radius of the reduced section was increased, and where sample edges were further polished fatigue life was improved even further [11]. In context, this seems to suggest that thinner material provides better fatigue life due to the small number of grains and limited opportunity for transgranular cracking. The same study demonstrated improved life in polished specimens as the origin of the cracks was almost always an edge defect. This highlights the importance of edge quality and the necessity to investigate the effect of remote laser cutting on fatigue life. A decrease in fatigue life at elevated temperatures has been reported for silicon steel which is proposed to be due to a decrease in material strength at such temperatures reducing the critical crack length [11]. Another investigation of slightly thicker sheets of 0.27 mm at a slightly lower temperature of 150 °C reported a decrease in fatigue life at  $10^4$  cycles [12] while [11] noted this behaviour at  $10^6$  cycles, but not at  $10^5$  cycles. The lower temperature of the former study combined with the thicker sample size further shows the significance of the size effect, one should expect the lower temperature study to report higher fatigue life in comparison to a higher temperature study. As the only major difference was the sample thickness, the relative influence of grain size to sheet thickness is highlighted as a dominant factor in the failure. The quality of the cut edge is an important factor because

in all cases in the aforementioned study the crack is initiated from the burr, due to the presence of microcracks propagating into the specimen. In a study on aluminium cut with a conventional laser cutting process, the striation wavelength was shown to have significant influence on the mechanical properties, in particular the fatigue life, but also factors such as the UTS [13]. Due to the differing material removal mechanism between CLC and RLC such regular striations are not expected, but the importance edge quality is once again highlighted, both geometrically (surface geometry) and in terms of resulting internal stresses.

Flux redistribution due to cut edge damage is a known phenomena in silicon steel; the magnetically damaged region may extend up to 15 mm from the cut edge depending upon exact material type [14,15]. A model for the permeability change due to laser cutting of CoFe showed flux redistribution may be an important factor in modelling loss in electrical machines [16]. A double exponential function was shown to describe the relative permeability at a given distance from the cut edge for one laser power parameter in conventional laser cutting. Therefore, it is not valid to assume the samples can be uniformly magnetised in the testing apparatus, such a finding has potentially severe implications on the energy loss due to edge damage for in service components. As such a sinusoidal voltage, as opposed to a sinusoidal induction, may be more representative of in situ components, due to flux redistribution effects invalidating assumptions about the induction state of any one localised material volume.

The present paper aims to investigate the effect of remote laser cutting, for the first time, on the magnetic and mechanical properties of commercial thin electrical steel sheets. The influence of laser power and consequent thermal damage accumulation on the magnetic permeability, tensile and fatigue properties were studied. This characterisation is important due to the lack of literature available for the RLC process on magnetic materials, as previously discussed, the mechanism of material removal differs significantly from that of CLC. The paper introduces a specific loss prediction criteria based on the perimeter of the cut edge, frequency, induction, and sheet direction (rolling or transverse directions) which is obtained by a linear regression.

## 2. Methodology

A commercial silicon steel, Tata Steel HiLite NO20, with a silicon content of 3.2% and a Suralac S9000 coating with an approximate thickness of 4.5  $\mu\text{m}$  was used in this study. The nominal chemical composition is provided in Table 1. A selected number of samples were prepared with standard metallographic practice to measure the grain size at the cross-section of the sheets. The nominal grain size was found to be 150  $\mu\text{m}$ , with two to five grains across the thickness. All samples were prepared using a single-mode fibre laser emitting at 1075.2 nm with a spot size of approximately 35  $\mu\text{m}$ , with a nominal traverse speed of 5  $\text{m s}^{-1}$  achieved using a high-speed galvanometer scanner. Two power levels of 1 kW and 2 kW were chosen based upon initial screening tests for acceptable cut quality. A cut through the full sheet thickness was achieved in 4 successive passes for the 1 kW power level. The 2 kW the beam did not typically require 4 passes to penetrate the material. This number of passes ensured all material was fully ejected from the cut. The subsequent passes were made immediately after one another, with no delay, to replicate an industrial approach and account for a potential heat build up. Multiple passes are used in order to ensure that material is primarily vaporised as opposed to melted, and that ejecta from the cut does not deflect the laser.

### 2.1. Effects of laser power on tensile properties

The effect of laser power on structural integrity of the cut materials was tested via the quasi-static tensile properties and the deformation to failure in uniaxial mechanical tests. Sub-sized tensile specimens were manufactured according to the ASTM-E8 standard using the selected laser powers of 1 kW and 2 kW and tested in the rolling, transverse, and

**Table 1**  
Normalised composition of material.

Element	Content (wt%)	Element	Content (wt%)
C	0.00245	Cu	0.023
Si	3.23	Mo	0.001
Mn	0.17	Al	1.06
P	0.019	Nb	0.002
S	0.001	Ti	0.008
N	0.0017	V	0.004
Cr	0.025	Ni	0.01

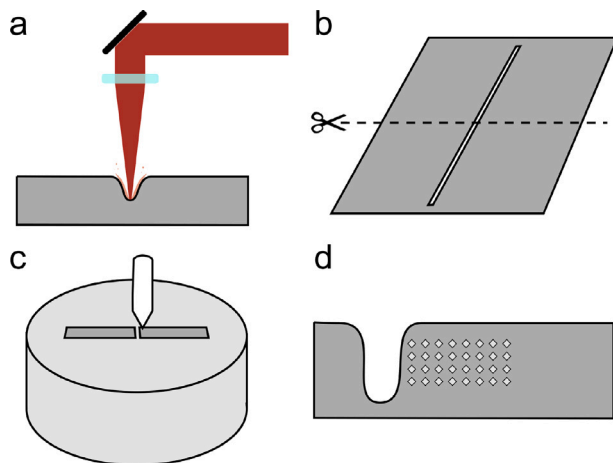


**Fig. 1.** Edge hardness measurement methodology. a: Laser cut is made, b: Sample is cut through centre, c: Sample is mounted, ground and polished, d: Indents through cross-section are acquired.

45° directions — to ensure any anisotropic behaviour was captured. A Tinius Olsen H25KS universal testing machine was used to perform the tests at a displacement rate of  $1 \text{ mm s}^{-1}$ . Digital image correlation (DIC) was used to obtain a full field deformation map on samples covered with a fine speckle pattern. The captured images were analysed using a physical subset size of  $0.344 \text{ mm}$  and a step size of one third of the subset size to obtain the displacement field from which the strain distribution and average strain over the gauge length could be determined using a virtual strain gauge of  $25 \text{ mm}$  as per the ASTM-E8 standard for sub-size specimens.

## 2.2. Effects of laser power on mechanical fatigue strength

Axial tension–tension fatigue tests were designed and conducted according to the ASTM fatigue testing standard [17] using the ASTM-E8 sample geometry used in Section 2.1. A Nene Instruments  $12 \text{ kN}$  servo-hydraulic testing machine was used to apply the sinusoidal loading pattern with a stress ratio (R) of zero and mean stresses,  $\sigma_m$ , ranging from  $160\text{--}300 \text{ MPa}$ . The tensile stress regime was selected as it resembles the applied stress state due to the centrifugal forces in an electric machine. The applied stress levels were selected according to yield stress of the material,  $\sigma_y = 395.8 \text{ MPa}$ , obtained from standard tensile tests to ensure the samples are loaded before and after the plastic yielding. As such the maximum force applied was  $600 \text{ N}$ , where  $\sigma_y$  is reached at  $475 \text{ N}$ . The total number of cycles to fracture was measured to determine the S-N curve for each case and the endurance limit was assumed for samples withstanding  $10^6$  cycles. Samples were tested as such that the loading was applied in line with the rolling direction.

In this study, compressive stress states are neglected for two motivations. Firstly, the material primarily experiences fluctuating sinusoidal tensile stresses during the service life due to the centrifugal forces. Secondly, samples will easily buckle under compressive stress states due to the sheet thickness from which they are manufactured. A force-controlled sinusoidal loading was therefore applied to replicate the

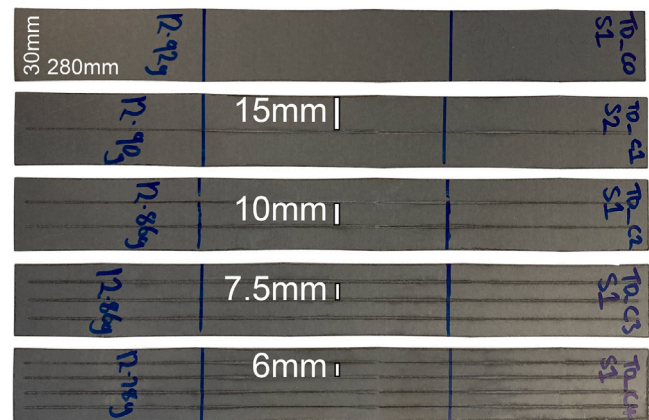


**Fig. 2.** A selection of samples with a varying number of slots, the blue lines indicate the section that was fully contained within the search coil of the single sheet tester.

in-service loads, which is also the suggested mode in the ASTM standard [17], although it is noted that different loading modes may have an effect in the fatigue life [18].

## 2.3. Effect of laser power on nanohardness

A hardness profile from the cut edge to the bulk material was measured via nanoindentation using a Hysitron TI Premier with a Berkovich tip. Cuts of varying power were made in a sheet and mounted in epoxy resin, which was then ground and polished to reveal access to the centre of the cut. A grid of 4 rows and 20 columns with a spacing of  $10.00 \mu\text{m}$  was indented, for a total measurement of  $200 \mu\text{m}$  from the cut edge (see Fig. 1). A trapezoidal load function with a peak force of  $1000 \mu\text{N}$ , a load and unload time of  $15 \text{ s}$  and a dwell time of  $60 \text{ s}$  was used. Samples with laser powers of ranging from  $250 \text{ W}$  to  $2000 \text{ W}$  were investigated, although due to rapid oxidation inadvertently effecting the results only the extreme values are reported.

## 2.4. Effects of laser power on magnetic performance

The influence of the laser parameters on the magnetic performance was investigated by calculating the specific loss of rectangular samples,  $30 \text{ mm} \times 280 \text{ mm}$ , tested in a single sheet tester (Laboratorio Elettrofisico AMH-1K Permeameter). Samples with an increasing number of cuts were produced using both the  $1$  and  $2 \text{ kW}$  laser powers and a nominal traverse speed of  $5 \text{ m s}^{-1}$ , producing equally spaced  $15$ ,  $10$ ,  $7.5$ , and  $6 \text{ mm}$  wide sections, connected at the both ends with  $5 \text{ mm}$  of remaining material as shown in Fig. 2. The tests were conducted at frequencies of  $200$ ,  $400$ , and  $1000 \text{ Hz}$  with a peak induction (B) of  $0.5$ ,  $1.0$  and  $1.5 \text{ T}$  each. These parameters were chosen to be representation of operating conditions. As some material is removed due to the cutting process, each sample was weighed before testing, and this post-cut weight was used in the calculation of the specific loss.

Slot samples were also generated using RLC, in this case some unwanted damage is introduced in the rectangular perimeter of the sample. As a consistent laser power setting was chosen for all perimeter cuts across all samples a true “zero loss” may be backwards extrapolated from the collected data if required, although only the relative increases are of interest in this study. Furthermore, although other methods such as wire EDM may have been used, it has been shown that this can still degrade properties as discussed in the introduction [5,6].

Both a sinusoidal magnetic induction and a sinusoidal voltage were trialled in some samples, and it was found the specific loss in both cases below magnetic saturation of the sample were similar, within  $5\%$ . The sinusoidal voltage method was therefore chosen because: the condition within an AC motor is a sinusoidal applied voltage (i.e. on the primary

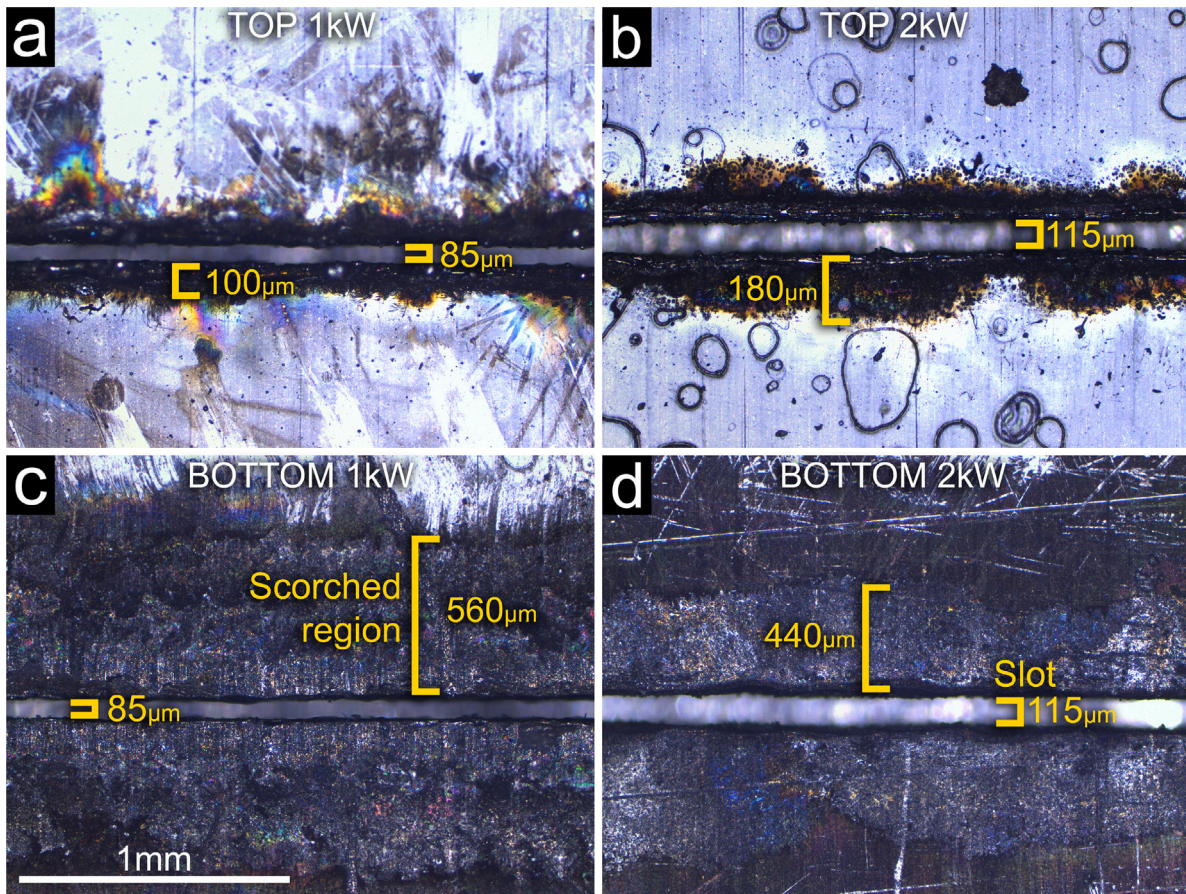


Fig. 3. Optical microscope images of the slots, (a) and (b) showing the front of the strip and (c) and (d) showing the back. Sub-figures (a) and (c) are cut at 1 kW and (b) and (d) at 2 kW. Typical dimensions of features are superimposed in yellow.

coil); the results are acquired much faster as no iterative scheme is required; and the trends in results at saturation are consistent using this method, whereas inconsistencies are developed in the iterative method above saturation, due to difficulty maintaining the required sinusoidal induction, particularly as the material becomes magnetically harder due to the induced damage from the laser cutting process. The distinction is made because using this scheme Section 4.4.3 of BS EN IEC 62044-3:2023 may be violated, particularly at saturation.

This methodology therefore is suitable for assessing investigation of the relative increase in specific loss with increasing damaged perimeter, but is not applicable for use with models requiring “base” magnetic properties, as these are typically formulated assuming a sinusoidal induction [19]. The aforementioned operating conditions within typical motor designs bolsters the justification as real world operating conditions are of greater interest to electric vehicle manufacturers.

As is later discussed in the results section, the material is magnetically saturated at an induction intensity ( $B$ ) of approximately 1.4T. The requested intensity was therefore chosen to be 1.5T — in this manner every sample can be guaranteed to have saturated and the difference in induction is increased consistently by 0.5T at every step. Again, such a methodology is in fact preferable when considering industrial applicability because as the material becomes magnetically harder it is expected that localised areas will behave differently to the bulk/undamaged regions. A simple metric for loss per damaged perimeter/area is desired which may otherwise be confused by a sinusoidal induction, due to flux redistribution effects etc.

### 3. Results

Fig. 3 displays a collage of images of the cut edge using optical microscopy. The typical width of cut was slightly increased with increased

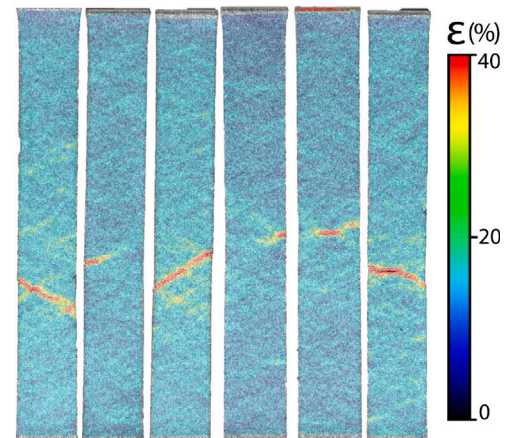
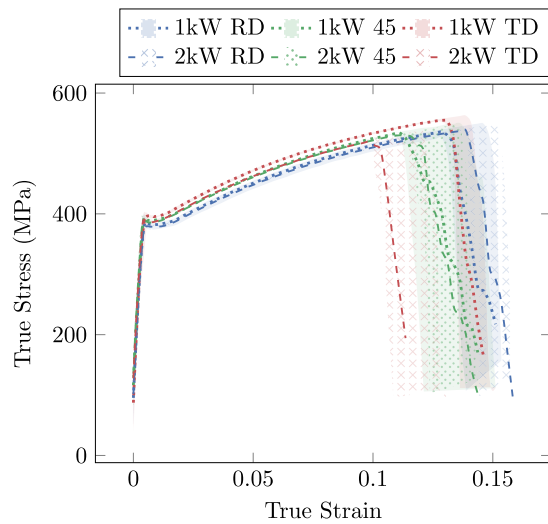


Fig. 4. Local strain distribution at the onset of fracture for a randomly selected set of samples demonstrating a maximum normal strain as high as 40 percent can be achieved at the onset of fracture with the applied DIC parameters.

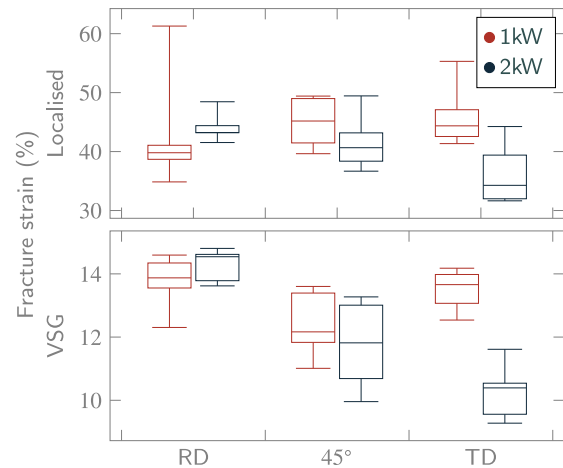
laser power, from an average of approximately 100  $\mu\text{m}$  to 130  $\mu\text{m}$ . Note also that because of the working principle of remote laser cutting the top surface of the samples show less heat damage from the laser, with the channel being slightly wider at the top. The bottom surface shows a large scorched area due to the accumulation of heat at each pass.

#### 3.1. Effect of laser power on tensile deformation and fracture

Fig. 5(a) shows the true stress–strain curves for each parameter while the corresponding deformation maps demonstrate the maximum



(a) Averaged true stress-strain curves for all samples, with minimums and maximums denoted by the shaded areas.



(b) Boxplot of maximum normal strain at fracture with respect to the laser power as well as loading directions, whiskers indicate minimum and maximum values.

Fig. 5. Results related to the quasi static tensile testing of the RLC NO20 material.

normal strain (log strain tensor) in Fig. 4. Fig. 5(a) displays an averaged value over all samples per type, with the maximum and minimum values represented by the shaded areas, allowing direct comparison to the boxplot displayed in Fig. 5(b). It was found that, for the parameters tested, the variation of laser power does appear to have an observable effect on the strain at fracture, although bulk properties in the elastic and plastic regions remain unchanged. Both the localised and 25 mm virtual strain gauge show decreased fracture strain in the transverse direction, the responsible mechanism is not yet clear. The microstructure of equiaxed grains without a preferred crystallographic orientation may be altered by the laser at the cut edge, alternatively, thermally induced residual stresses may also have some effect, further investigation is required.

A strain map for several samples, indicating the maximum normal strain at fracture, is shown in Fig. 4. Prior to fracture, a non uniform strain field develops due to the plastic deformation. Fig. 5(b) shows a box plot comparing the maximum normal strain at fracture for samples cut in the rolling direction (RD), transverse direction (TD) and at 45°. Although each population contains high variance, the mean fracture strain appears to be lower for samples cut in the transverse direction. The variance can be explained primarily by the so-called size effect. The average diameter of the grains is 150  $\mu\text{m}$  meaning that a typical 0.2 mm thick sample has 1 to 3 grains through its thickness, which produces a deformation which cannot be approximated as a continuum. The size effect dominates the fracture dynamics, and any heat affected zone (HAZ) at the edge is insignificant in comparison. The mechanism of fracture is proposed to be intergranular cleavage, as seen in Fig. 4 strain localisation is developed in bands at approximately 25° to 35° with respect to the tensile axis, a crack initiates at the edge due to this induced stress concentration, which promotes plastic deformation along the band in the direction of the localised band. This produces a characteristic tearing-type fracture, consistent with samples produced by EDM and waterjet cutting. Such a mechanism is strengthened by the higher power level inducing higher residual stresses at the cut edge. Some samples show centre-initiated fracture, as opposed to edge initiated, in such cases the localisation occurs much more severely (i.e. the strain gradient is higher).

### 3.2. Effect of laser power on cycles to failure

No fatigue fracture was observed for the samples tested with a peak stress below the yield strength of the material  $\sigma_y = 395.8 \text{ MPa}$  and  $r = 0$ .

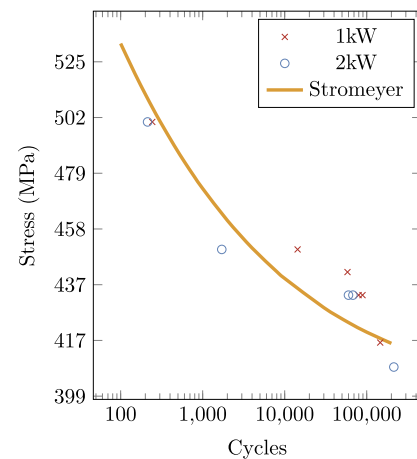


Fig. 6. SN curve comparison between laser power levels. Red crosses indicate samples 1 kW laser power level samples and blue circles 2 kW. The Stromeier fatigue life model is plotted as a yellow line.

Fig. 6 shows results for both laser power parameters and the Stromeier model [20] for fatigue life is plotted for  $C = 13.77$ ,  $\sigma_w = 395.8 \text{ MPa}$ . The fit for this model achieved an R-Square value of 0.80 .

Using a one way ANOVA the laser power level was found to be an insignificant factor at the  $p = 0.05$  level suggesting the laser power was not an influence in the fatigue life. Further testing at differing stress ratios may be of interest but could not be completed in this study due to equipment limitations.

### 3.3. Effect of laser power on nanohardness

The nanohardness was measured from the cut edge into the bulk material, an example of the positioning of the indented region is shown in Fig. 9. Fig. 7 shows the results of nanohardness measurements near the cut edge. Increased hardness is observed at the cut edge, with higher laser power producing an increased hardness. Interestingly, higher laser power also produced more variability in the hardness at the cut edge, as shown in Fig. 7, with the region within the first 30  $\mu\text{m}$  from the cut edge having greatest range in measured values. Residual

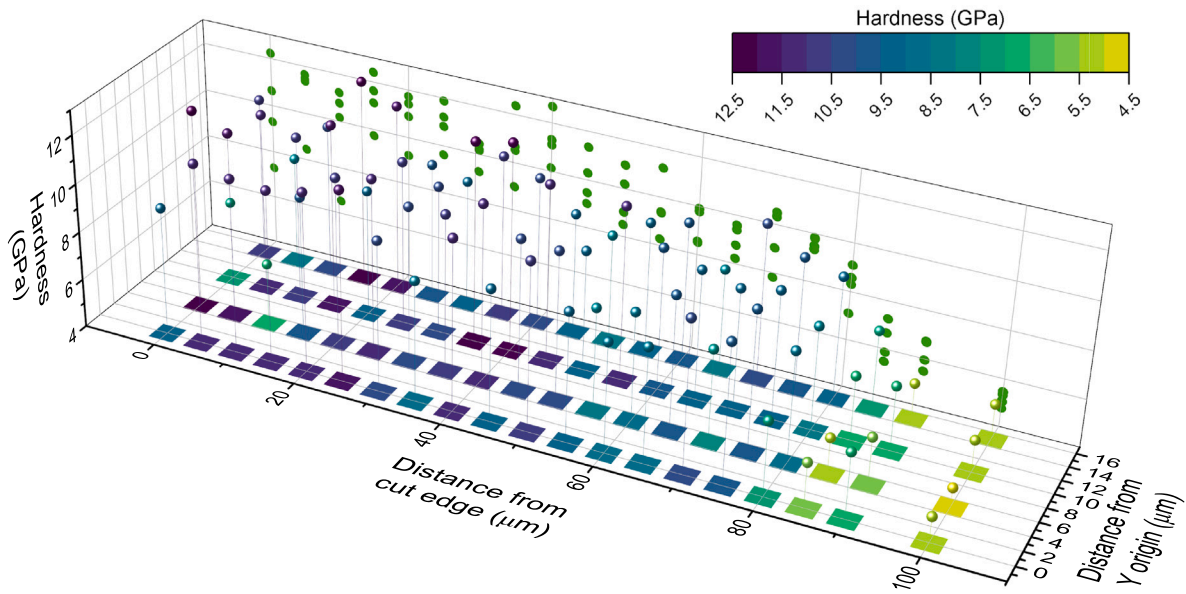


Fig. 7. A three dimensional plot of the nanohardness observed for one sample. The x axis indicates the distance from the cut edge, 4 rows of indents are visible. Fig. 8 simplifies this figure by averaging the hardness between rows.

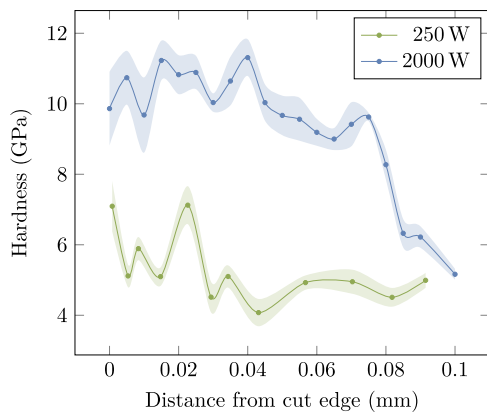


Fig. 8. A comparison of the hardness at the cut edge, the solid line indicates the mean average hardness over the measurement area, and the shaded area shows the standard error. The bulk material hardness was measured as approximately 4 GPa, in agreement with other studies [21].

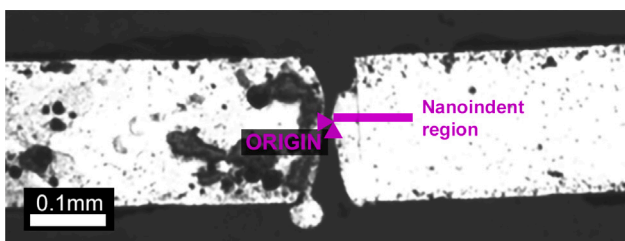


Fig. 9. Location of the nanoindent region on a sectioned sample.

stresses in the microstructure may explain both the increased hardness and increased variance. To combat this variability the average of 4 hardness measurements across the 40 μm strip of indents is shown in Fig. 8, and a comparison between two extremes of power is made. In both cases the hardness in the vicinity of the cut edge is increased.

The nanohardness at the cut edge is shown to increase compared to the bulk hardness, the effect displayed for approximately 0.08 mm from the cut edge for a laser power of 2000 W. The visually altered remelt

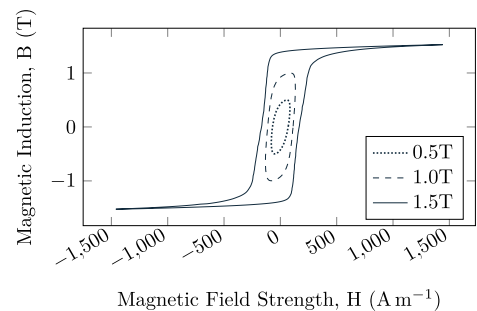


Fig. 10. Three superimposed hysteresis loops at various magnetic induction values, B, for an RD sample with no cuts at 1000 Hz. This form is typical of all tested samples at all frequencies, with the loop “softening” at lower frequencies as demonstrated in Fig. 11.

zone of the metal is significantly smaller than this, although as noted in Fig. 3 the coating becomes damaged as much as 0.5 mm from the slot. It is noted that the increased hardness due to laser cutting is not present after 0.1 mm, after which the bulk material hardness is measured.

It is possible that the hardness profile varies across the thickness of the sheet, although in this study the central region was chosen as a representative average area. As shown in Fig. 3 the bottom of the sheets appears scorched across a much larger area than the top — although the bottom scorched region is significantly larger (approximately 5×) than the region of increased hardness.

### 3.4. Effect of laser power on specific loss

Figs. 11 and 10 show hysteresis loop comparisons across various samples and working points, the former compares 0, 2, and 4 slot samples at the extremes of the working points of 200 Hz to 1000 Hz and 0.5T to 1.5T. Samples with 1 and 3 slots have been excluded for clarity of the figure. Fig. 10 shows the hysteresis loops for the three induction values tested for a 0 slot sample at 1000 Hz. From these figures it is clear that the samples were effectively saturated at approximately 1.4T, although 1.5T was ultimately reached as this was the requested value during the test. In this article further reference to

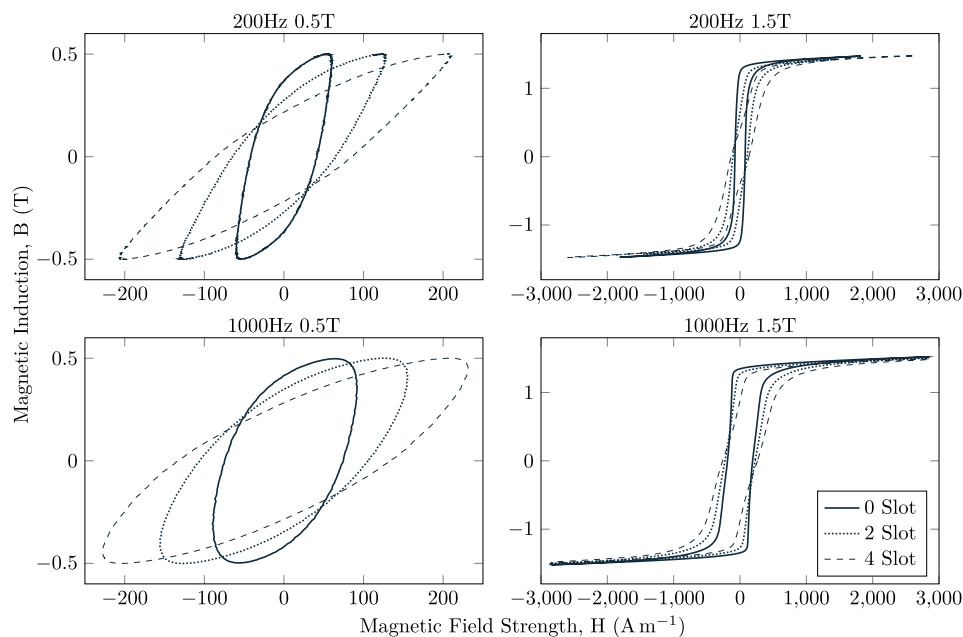


Fig. 11. Hysteresis loop comparison between 0 and 4 slot samples at the maximum and minimum working points of 200–1000 Hz and 0.5–1.5T.

saturation should be understood as the field values above the knee-point, providing technical/effective saturation. The measured specific loss as a function of the number of cuts for different frequencies, and the magnetic flux, are shown in Figs. 12(a) and 12(b) for samples cut using 1 kW and 2 kW laser, respectively. The crosses correspond to the frequency of 200 Hz while hollow and solid circles are the magnetic measurement results at 400 and 1000 Hz, for all samples, respectively. The specific loss increases linearly with the number of cuts regardless of the testing conditions, as it is shown in Figs. 12(a) and 12(b). As such, it is evident that any loss or flux redistribution effects are fully contained within 3 mm, half the minimum spacing between cuts. The perimeter of the cut drives the loss for any particular working condition, a “damaged perimeter coefficient” for any working point can therefore be found by linear regression, multiplying the number of slots by the slot length. In all cases samples where the slots were made in the transverse direction exhibited higher losses by an average of 24%.

The zero slot sample’s specific loss can be taken as a reference value from which the influence of additional damage due to the slots is calculated. The zero slot samples in all cases were cut using the 1 kW parameter, as such the relative increase in loss can be considered. It is clear from Figs. 12(a) and 12(b) that for any given parameter combination of induction and frequency a linear regression may be made to predict the additional loss due to damage from the laser cutting process. The number of slots is transformed into “damage perimeter” by multiplying the number of slots by twice the mean free path (108 mm \* 2) inside the single sheet tester, because each slot produces two damaged edges. The 0 slot loss is subtracted from the loss values for slotted samples in the same group, producing a value of *additional loss* as a result of the perimeter of the cut edge. A linear regression is performed on the slotted sample values with the intercept forced to 0. The resulting slope therefore is the increase in specific loss per cut edge perimeter, in  $\text{W kg}^{-1} \text{m}^{-1}$ , and this normalised value is useful for visualisation and modelling purposes because of the reduced dimensionality. Fig. 13 shows the normalised loss value against the induction and frequency of the samples tested in the rolling direction. Here it is possible to see the effect of non-linearity in the normalised loss values due to the changing frequency and induction, and indeed this trend is also present in the 0 slot samples.

True undamaged samples were manufactured by wire electrical discharge machining (WEDM), as a comparison point against the 0

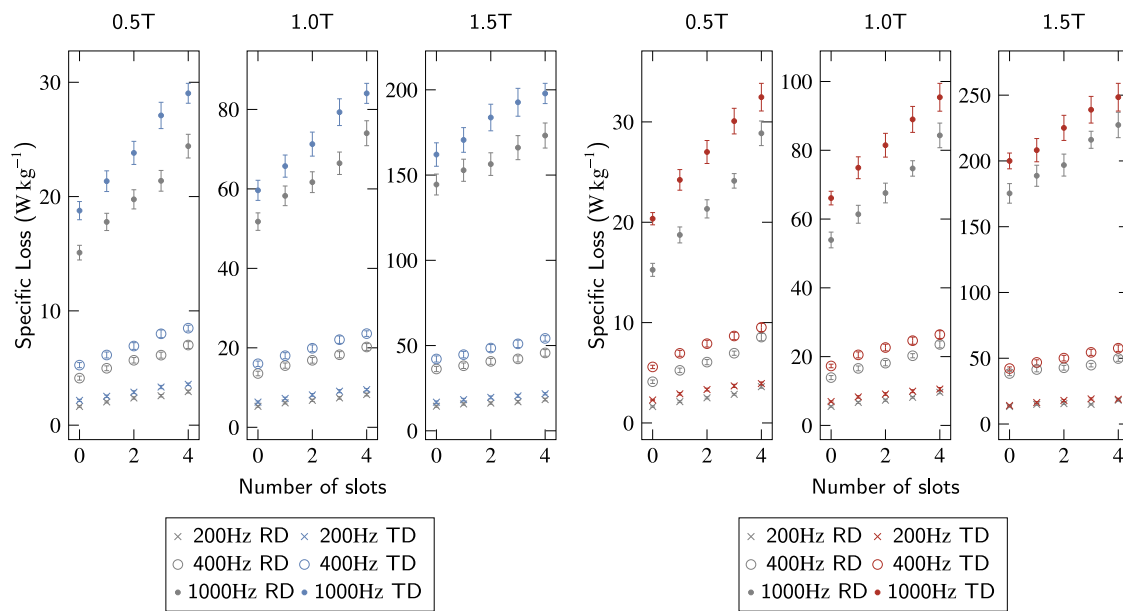
slot samples manufactured with RLC. Table 2 shows the results for an RD sample. Notably the zero slot samples have a significantly higher loss than the true undamaged samples at the highest induction, even after correcting for the two laser cut edges by extrapolating using the calculated normalised loss. The possible source of the errors are now discussed: at low inductions the sensitivity to the regression is higher due to the low values, as such the regression is more influenced by deviation from the mean in the dataset. Further increasing the number of samples in the dataset could reduce any such influence. At higher inductions the material is operating at technical saturation and the influence of degraded magnetic performance is much higher on the specific loss — although after the initial damage occurs further damaging the material produces a linear increase in specific loss, the initial damage process is likely highly non linear.

The figures displayed in Table 2 for the WEDM samples agree well with the manufacturer specified values for the material, further validating the methodology applied to the RLC samples.

It may be noted that due to equipment limitations it was not possible to record the magnetic field strength, H, beyond  $2800 \text{ A m}^{-1}$ . As the material was saturated before this point this is deemed inconsequential for the results presented in this section — specific loss is calculated according to the area inside the hysteresis loop and the region after saturation is extremely small by comparison. The measurement and achievement of the requested induction, B, is not affected by this limitation.

#### 4. Conclusions

This paper has shown there is little bulk mechanical difference in the plastic region of the material response between the laser power level used for the parameter sets tested in RLC, suggesting any number of passes and any laser power may be expected to produce parts with equal bulk mechanical quality. A difference was observed in edge hardness and fracture strain between the parameters, notably as the sample orientation had a greater transverse component the fracture strain decreased at higher power. This is indicative of the important role the edge quality has on the fracture strain — residual stresses at the cut edge or poor geometric accuracy can initiate a crack. Interestingly this finding did not translate to the cycles to failure, both parameters gave essentially equivalent fatigue life. This may be due to an insufficient



(a) 1kW RLC samples. A linear relationship is apparent under all testing conditions. (b) 2kW RLC samples. Again, a linear relationship between specific loss and number of slots is observed.

Fig. 12. Specific loss as a function of the number of cuts in the material, presented at various field inductions and frequencies.

Table 2

Predicted vs actual undamaged loss based upon linear regression for 1kW remote laser cut rolling direction samples.

Frequency (Hz)	Induction (T)	Undamaged Loss ( $W\ kg^{-1}$ )	Predicted 0 slot Loss ( $W\ kg^{-1}$ )	Actual 0 slot Loss ( $W\ kg^{-1}$ )	Difference (%)
200	0.5	1.24	1.90	1.64	-16
400	0.5	3.17	4.61	4.11	-12
1000	0.5	12.19	16.7	15.3	-9.7
200	1.0	4.17	5.65	5.52	-2.3
400	1.0	11.0	14.3	13.9	-2.9
1000	1.0	43.3	53.9	53.9	0.0
200	1.5	10.9	12.7	13.3	4.1
400	1.5	28.3	32.7	38.4	14
1000	1.5	109	123	175	30

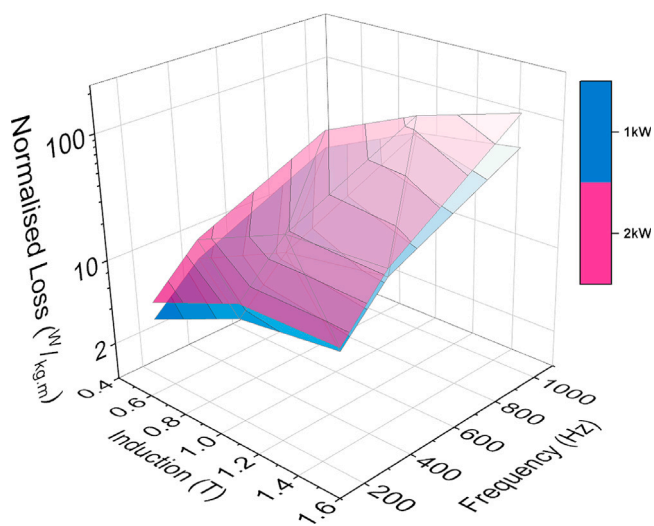


Fig. 13. Normalised loss plotted against frequency and induction for 1 and 2 kW samples in the rolling direction.

dataset for cycles to failure, but because the material does not exhibit low cycle fatigue at all (in both this study and the literature) such minor edge effects between the two parameter sets tested are likely insignificant in comparison to localised and stochastic hardening in the plastic region. The edge hardness was observed to increase with a higher power producing a higher hardness over a larger distance from the cut edge. Bulk material hardness was reached within one sheet thickness in the highest laser power case, significantly smaller than all practical features of a part manufactured for use in today’s electrical machines. Using this knowledge, manufacturers are free to optimise remote laser cutting for the preservation of the magnetic qualities. In comparison to results for guillotine and blanked edges as investigated by Wu et al. [22] RLC offers a smaller region of increased hardness with a significantly sharper gradient between affected and unaffected regions. Such an affect is primarily due to plastic strain developed in mechanically cut samples which is not present in laser cut samples. This study also found the thermally affected zone to be much smaller than that of a CLC as reported in [7] of 1600  $\mu m$  from the cut edge, although it is noted that due to the age of this study the material used had a significantly different microstructure which is likely to cause such a difference.

This study has shown that the magnetic loss is a linear function of damage perimeter, down to the minimum tested slot separation of 6 mm. It is likely that the increased hardness occurring at the cut edge is indicative of the magnetically damaged region, meaning a minimum

spacing of the order of 0.2 mm would be required to see non-linear loss increases. Higher losses were observed in samples produced with higher laser power, suggestive of heat damage due to the energy of the laser heating but not fully vaporising the material. This counter-intuitive affect may be due to the vaporised material being unable to exit the cut fully at higher volumes, however the complex interaction of laser power, scan speed, and absorptivity (particularly at phase transitions) mean further work is required to fully characterise such an observation. An alternative explanation is that above approximately  $10 \times 10^8 \text{ W cm}^{-2}$  a plasma is formed that prevents beam absorption [23], if such plasma re-radiates even a fraction of the energy to part the potential for significant heating is present.

Although the material is designed to be isotropic, an increased loss was observed in samples manufactured in the transverse direction. Upon normalisation a difference between transverse and rolling direction samples was still observable in some conditions, with transverse samples showing increased influence of damage perimeter on loss. At higher frequency and induction this may be an important factor in the cooling requirements of electric machines — as heat generation may be higher in cuts aligned with the transverse direction.

Based on the parameters selected RLC significantly degrades the magnetic performance and is not deemed a viable method for lamination cutting. Refinement of the laser parameters and/or the use an alternative laser such as an ultra-fast pulsed laser is required to be competitive with existing methods such as CLC or blanking. One study suggests nanosecond pulse laser processing may be viable to maintain magnetic qualities [24], however a significantly reduced power of 17 W at a speed of at  $0.5 \text{ m min}^{-1}$  was used. Despite the increased loss, the speed of RLC remains an attractive quality for which further investigation is merited.

#### CRediT authorship contribution statement

**L.M. Jones:** Writing – review & editing, Writing – original draft, Visualization, Validation, Resources, Project administration, Methodology, Investigation, Formal analysis, Data curation, Conceptualization. **A. Winter:** Writing – review & editing, Validation, Resources, Methodology, Investigation, Conceptualization. **L. Tinkler:** Writing – review & editing, Resources, Methodology, Conceptualization. **G.W. Jewell:** Writing – review & editing, Supervision, Project administration, Funding acquisition. **H. Ghadbeigi:** Writing – review & editing, Supervision, Project administration, Conceptualization.

#### Declaration of competing interest

The authors declare that they have no known competing financial interests or personal relationships that could have appeared to influence the work reported in this paper.

#### Data availability

Data will be made available on request.

#### Acknowledgements

This work is supported by the UK Engineering and Physical Sciences Research Council (EPSRC) through funding for the Future Electrical Machines Manufacturing Hub (Award EP/S018034/1).

#### References

- [1] A. Krings, C. Monissen, Review and trends in electric traction motors for battery electric and hybrid vehicles, in: 2020 International Conference on Electrical Machines, ICEM, IEEE, ISBN: 978-1-7281-9945-0, 2020, pp. 1807–1813, <http://dx.doi.org/10.1109/ICEM49940.2020.9270946>, URL <https://ieeexplore.ieee.org/document/9270946/>.
- [2] SCHULER GmbH, Metal Forming Handbook, Springer Berlin Heidelberg, Berlin, Heidelberg, ISBN: 978-3-642-63763-6, 1998, <http://dx.doi.org/10.1007/978-3-642-58857-0>, URL <http://link.springer.com/10.1007/978-3-642-58857-0>.
- [3] A. Wetzig, J. Hauptmann, P. Herwig, E. Beyer, W. Bundschuh, S. Volk, M. Hemberger, Inline high speed laser cutting of band material, in: Materials Science Forum, 854, Trans Tech Publications Ltd, (ISSN: 16629752) ISBN: 9783038356158, 2016, pp. 237–242, <http://dx.doi.org/10.4028/www.scientific.net/MSF.854.237>.
- [4] A. Winter, L. Tinkler, G.W. Jewell, Remote laser cutting of high cobalt content electrical steel: preliminary results and microscopy, in: 11th International Conference on Power Electronics, Machines and Drives, PEMD 2022, Institution of Engineering and Technology, ISBN: 978-1-83953-718-9, 2022, pp. 708–711, <http://dx.doi.org/10.1049/icp.2022.1141>, URL <https://digital-library.theiet.org/content/conferences/10.1049/icp.2022.1141>.
- [5] V.M. Paltanea, G. Paltanea, H. Gavrilă, Some important effects of the water jet and laser cutting methods on the magnetic properties of the non-oriented silicon iron sheets, in: 2015 9th International Symposium on Advanced Topics in Electrical Engineering, ATEE 2015, Institute of Electrical and Electronics Engineers Inc., ISBN: 9781479975143, 2015, pp. 452–455, <http://dx.doi.org/10.1109/ATEE.2015.7133856>.
- [6] G. Paltanea, H. Gavrilă, The effect of mechanical and electrical discharge cutting technologies on the magnetic properties of non-oriented silicon iron steels electromagnetic levitation for sensors view project, 2015, pp. 59–68, URL <https://www.researchgate.net/publication/283021227>.
- [7] A. Belhadj, P. Baudouin, F. Breaban, A. Deffontaine, M. Dewulf, Y.H.R.C. Sambre, Effect of laser cutting on microstructure and on magnetic properties of grain non-oriented electrical steels, 256, 2003, pp. 20–31.
- [8] B. Silwal, P. Sergeant, Thermally induced mechanical stress in the stator windings of electrical machines, Energies (ISSN: 19961073) 11 (2018) <http://dx.doi.org/10.3390/en11082113>.
- [9] B. Bode, F. Zeismann, A. Brückner-Foit, Fatigue behaviour of electrical steel, in: MATEC Web of Conferences, Vol. 12, EDP Sciences, (ISSN: 2261236X) ISBN: 9782759812745, 2014, <http://dx.doi.org/10.1051/mateconf/20141204019>.
- [10] A. Gottwalt, P. Kubaschinski, M. Waltz, U. Glatzel, U. Tetzlaff, An experimental setup for fatigue testing of thin electrical steel sheets, Int. J. Fatigue (ISSN: 01421123) 162 (2022) <http://dx.doi.org/10.1016/j.ijfatigue.2022.106987>.
- [11] H. Dehmani, C. Brugger, T. Palin-Luc, C. Mareau, S. Koechlin, S.K. High, Cycle fatigue strength of punched thin Fe-Si steel sheets. Materials performance and characterization 5, 2016, pp. 1–15, <http://dx.doi.org/10.1520/MPC20150063>, URL <https://hal.science/hal-01375905>.
- [12] G. Gill, B. Behraves, D. Saha, W. Zhang, J. Chen, G. Lamonaca, M. Mills, H. Jahed, Fatigue behavior of stamped electrical steel sheet at room and elevated temperatures, 2023, <http://dx.doi.org/10.4271/2023-01-0804>, URL <https://www.sae.org/content/2023-01-0804>.
- [13] S. Ullah, X. Li, G. Guo, A.R. Rodríguez, D. Li, J. Du, L. Cui, L. Wei, X. Liu, Influence of the fiber laser cutting parameters on the mechanical properties and cut-edge microfeatures of a AA2B06-T4 aluminum alloy, Opt. Laser Technol. (ISSN: 00303992) 156 (2022) 108395, <http://dx.doi.org/10.1016/j.optlastec.2022.108395>.
- [14] R. Rygal, A. Moses, N. Derebasi, J. Schneider, A. Schoppa, Influence of cutting stress on magnetic field and flux density distribution in non-oriented electrical steels, J. Magn. Magn. Mater. (ISSN: 03048853) 215–216 (2000) 687–689, [http://dx.doi.org/10.1016/S0304-8853\(00\)00259-6](http://dx.doi.org/10.1016/S0304-8853(00)00259-6).
- [15] A. Moses, N. Derebasi, G. Loisos, A. Schoppa, Aspects of the cut-edge effect stress on the power loss and flux density distribution in electrical steel sheets, J. Magn. Magn. Mater. (ISSN: 03048853) 215–216 (2000) 690–692, [http://dx.doi.org/10.1016/S0304-8853\(00\)00260-2](http://dx.doi.org/10.1016/S0304-8853(00)00260-2).
- [16] X. Chen, H. Wu, J.D. Ede, G.W. Jewell, L.M. Jones, H. Ghadbeigi, A model to account for magnetic permeability changes resulting from edge damage caused by laser cutting in a high performance cobalt-iron alloy, J. Magn. Magn. Mater. (ISSN: 03048853) 584 (2023) <http://dx.doi.org/10.1016/j.jmmm.2023.171081>.
- [17] ASTM, Standard Practice for Conducting Force Controlled Constant Amplitude Axial Fatigue Tests of Metallic Materials 1. <http://dx.doi.org/10.1520/E0466-15>. URL [www.astm.org](http://www.astm.org).
- [18] M. Gong, I. Smith, Effect of waveform and loading sequence on low-cycle compressive fatigue life of spruce, J. Mater. Civ. Eng. (ISSN: 0899-1561) 15 (2003) 93–99, [http://dx.doi.org/10.1061/\(ASCE\)0899-1561\(2003\)15:1\(93\)](http://dx.doi.org/10.1061/(ASCE)0899-1561(2003)15:1(93)), URL <https://ascelibrary.org/doi/10.1061/%28ASCE%290899-1561%282003%2915%3A1%2893%29>.
- [19] G. Bertotti, A. Boglietti, M. Chiampi, D. Chiarabaglio, F. Fiorillo, M. Lazzari, An improved estimation of iron losses in rotating electrical machines, IEEE Trans. Magn. (ISSN: 0018-9464) 27 (1991) 5007–5009, <http://dx.doi.org/10.1109/20.278722>.
- [20] C.E. Stromeyer, S.B. Baker, H. All, The determination of fatigue limits under alternating stress conditions, Proc. R. Soc. Lond. Ser. A Contain. Pap. Math. Phys. Charact. (ISSN: 0950-1207) 90 (1914) 411–425, <http://dx.doi.org/10.1098/rspa.1914.0066>, URL <https://royalsocietypublishing.org/doi/10.1098/rspa.1914.0066>.

- [21] H. Ghadbeigi, A. Al-Rubaye, F.C. Robinson, D. Hawezy, S. Biroasca, K. Atallah, Blanking induced damage in thin 3.2% silicon steel sheets, *Prod. Eng.* (ISSN: 18637353) 14 (2020) 53–64, <http://dx.doi.org/10.1007/s11740-019-00931-1>.
- [22] F. Wu, L. Zhou, J. Soulard, B. Silvester, C. Davis, Quantitative characterisation and modelling of the effect of cut edge damage on the magnetic properties in NGO electrical steel, *J. Magn. Magn. Mater.* (ISSN: 03048853) 551 (2022) 169185, <http://dx.doi.org/10.1016/j.jmmm.2022.169185>.
- [23] W.M. Steen, *Laser Material Processing*, Springer-Verlag, New York ; Berlin ; London, ISBN: 0387196706, 1991.
- [24] K. Winter, Z. Liao, R. Ramanathan, D. Axinte, G. Vakil, C. Gerada, How non-conventional machining affects the surface integrity and magnetic properties of non-oriented electrical steel, *Mater. Des.* (ISSN: 02641275) 210 (2021) 110051, <http://dx.doi.org/10.1016/j.matdes.2021.110051>.